CORE
Metadata, citation and similar papers at core.ac.uk
Provided by IntechOpen

We are IntechOpen, the world's leading publisher of Open Access books Built by scientists, for scientists

4,800
Open access books available

122,000
International authors and editors

135M
Downloads

Our authors are among the

154
Countries delivered to

TOP 1%
most cited scientists

12.2%
Contributors from top 500 universities

WEB OF SCIENCE™

Selection of our books indexed in the Book Citation Index in Web of Science™ Core Collection (BKCI)

Interested in publishing with us?
Contact book.department@intechopen.com

Numbers displayed above are based on latest data collected.
For more information visit www.intechopen.com

Chapter 14

Numerical Modeling of Flow and Sediment Transport in Lake Pontchartrain due to Flood Release from Bonnet Carré Spillway

Xiaobo Chao, Yafei Jia and A. K. M. Azad Hossain

Additional information is available at the end of the chapter

http://dx.doi.org/10.5772/54435

1. Introduction

Lake Pontchartrain is a brackish estuary located in southeastern Louisiana, United States. It is the second-largest saltwater lake in U.S. The lake covers an area of 1630 square km with a mean depth of 4.0 meters. It is an oval-shaped quasi-enclosed water body with the main east-west axis spanning 66 km, while the shorter north–south axis is about 40 km. It is connected to the Gulf of Mexico via Rigolets strait, to Lake Borgne via Chef Menteur Pass, and to Lake Maurepas via Pass Manchac. These lakes form one of the largest estuaries in the Gulf Coast region. It receives fresh water from a few rivers located on the north and northwest of the lake. The estuary drains the Pontchartrain Basin, an area of over 12,000 km^2 situated on the eastern side of the Mississippi River delta plain.

Lake Pontchartrain has served the surrounding communities for more than two centuries. The coastal zone of the Lake and its basin has offered opportunities for fishing, swimming, boating, crabbing and other recreational activities. The Lake Basin is Louisiana's premier urban estuary and nearly one-third of the state population live within this area. Over the past decades, rapid growth and development within the basin have resulted in significant environmental degradation and loss of critical habitat in and around the Lake. Human activities associated with pollutant discharge and surface drainage have greatly affected the lake water quality (Penland et al., 2002).

In order to protect the city of New Orleans from the Mississippi River flooding, the Bonnet Carré Spillway (BCS) was constructed from 1929 to 1936 to divert flood water from the river into Lake Pontchartrain and then into the Gulf of Mexico. However, a BCS opening event may cause many environmental problems in the lake. To evaluate the environmental im-

INTECH
open science | open minds

© 2013 Chao et al.; licensee InTech. This is an open access article distributed under the terms of the Creative Commons Attribution License (http://creativecommons.org/licenses/by/3.0), which permits unrestricted use, distribution, and reproduction in any medium, provided the original work is properly cited.

pacts of the flood water on lake ecosystems, it is important to understand the hydrodynamics as well as sediment transport in the lake.

Lake Pontchartrain is a large shallow lake and the water column is well mixed. In general, the water movements within the lake are affected by wind and tide. During the BCS opening for flood release, the flow discharge over the spillway produces significant effects on the lake hydrodynamics.

Numerical models generally are cost-effective tools for predicting the flow circulation and pollutant transport in a lake environment. In recent years, numerical models have been applied to simulate the flow and pollutant distribution in Lake Pontchartrain. Hamilton et al. (1982) developed a 2D-vertical integrated model to simulate the flow circulation in Lake Pontchartrain. The model is an explicit numerical difference scheme based on leap-frog integration algorithm, and a coarse uniform mesh with a spacing of 1 km was selected for numerical simulation. Signell (1997) applied the coastal and ocean model (ECOM), developed by Hydroqual to simulate the tide and wind driven circulation processes in the lake. It was found that water levels in Mississippi Sound influence the circulation patterns in the eastern part of the lake, while the wind force dominates the flow pattern of the western part. McCorquodale et al. (2005) applied a 3D coastal ocean model, ECOMSED, to simulate the flow fields and mass transport in Lake Pontchartrain. Dortch et al. (2008) applied the CH3D-WES hydrodynamic model, developed by the US Army Corps of Engineers, to simulate the lake flow field and post-Hurricane Katrina water quality due to the large amount of contaminated floodwater being pumped into the Lake. McCorquodale et al. (2009) developed a 1D model for simulating the long term tidal flow, salinity and nutrient distributions in the Lake. Most of those researches focus on hydrodynamics and pollutant transport in the Lake.

In this study, the flow fields and sediment transport in Lake Pontchartrain during a flood release from BCS was simulated using the computational model CCHE2D developed at the National Center for Computational Hydroscience and Engineering (NCCHE), the University of Mississippi (Jia and Wang 1999, Jia et al. 2002). This model can be used to simulate free surface flows and sediment transport, and the capabilities were later extended to simulate the water quality, pollutant transport and contaminated sediment (Chao et al. 2006, Zhu et al. 2008). CCHE2D is an integrated numerical package for 2D-depth averaged simulation and analysis of flows, non-uniform sediment transport, morphologic processes, water quality and pollutant transport. There are several turbulence closure schemes available within the model for different purposes, including the parabolic eddy viscosity, mixing length, k–ε and nonlinear k–ε models. A friendly Graphic User Interface (GUI) is available to help users to setup parameters, run the simulation and visualize the computational results. In addition to general data format, CCHE2D has capabilities to produce the simulation results in ArcGIS and Google Earth data formats (Hossain et al., 2011). Those capabilities greatly improve the model's applications.

The simulated flow and sediment distribution during the BCS opening were compared with satellite imagery and field measured data provided by the United States Geological Survey (USGS) and the United States Army Corp of Engineers (USACE). Good agreements were ob-

http://dx.doi.org/10.5772/54435

tained from the numerical model. This model provides a useful tool for lake water quality management.

2. Bonnet Carré Spillway (BCS) opening for flood release

In response to the high flood stage of the Mississippi River and to protect the city of New Orleans, the Bonnet Carré Spillway (BCS) was built to divert Mississippi River flood waters to the Gulf of Mexico via Lake Pontchartrain (Fig. 1).

Figure 1. The location of Bonnet Carré Spillway (BCS)

The construction of the spillway was completed in 1931. It is located in St. Charles Parish, Louisiana - about 19 km west of New Orleans. The spillway consists of two basic components: a 2.4 km long control structure along the east bank of the Mississippi River and a 9.7 km floodway that transfers the diverted flood waters to the lake. The design capacity of the spillway is 7080 m^3/s and will be opened when the Mississippi river levels in New Orleans approached the flood stage of 5.2 m. It was first operated in 1937 and nine times thereafter (1945, 1950, 1973, 1975, 1979, 1983, 1997, 2008 and 2011). The maximum flow discharges and days of opening for each event are listed in Table 1 (USACE 2011; GEC 1998).

During the BCS opening, a large amount of fresh water and sediment discharged from the Mississippi River into Lake Pontchartrain and then into the Gulf of Mexico. The flow discharge over the spillway produces significant effects on the lake hydrodynamics. It also changes the distributions of salinity, nutrients and suspended sediment (SS) in the lake dramatically. During a flood releasing event, the fresh water dominated the whole lake and the lake salinity reduced significantly. A lot of sediment deposited into the lake or was transported into the Gulf of Mexico. The contaminated sediment from Mississippi River could bring a lot of pollutants, such as nutrients, Al, Cu, Cr, Hg, Pb, Zn, etc., to the lake, and

caused a lot of environmental problems. The algal bloom occurred in a large area of the lake after a flood release event. The blooms produced high levels of heptatoxins and caused decreases of dissolved oxygen in the lake (Dortch et al., 1998; Penland et al., 2002).

Year	Date opened	Date Closed	Days opened	Max. discharge m^3/s
1937	Jan28	Mar 16	48	5975
1945	Mar 23	May 18	57	9005
1950	Feb 10	Mar 19	38	6315
1973	Apr 8	Jun 21	75	5522
1975	Apr 14	Apr 26	13	3115
1979	Apr 17	May 31	45	5409
1983	May 20	Jun 23	35	7589
1997	Mar 17	Apr 18	31	6881
2008	Apr 11	May 8	28	4531
2011	May 9	June 20	42	8892

Table 1. Information of Bonnet Carré Spillway opening for flood release

Due to a large amount of sediment discharged /deposited into the lake, the bed form of the lake changed. The BCS opening event produced significant changes in flow pattern, salinity and water temperature, which greatly affected the lake fish habitat, and caused negative impacts to oyster beds and fishery nursery grounds in the lake. In response to the dynamic changes in the salinity, temperature, water surface elevation, and bed form of the lake, it was observed that some species, particularly brown shrimp, shifted and moved. It may take a long time for the fisheries resources to recover from the flood release event.

To understand the impact of the BCS flood release event on the ecosystem of Lake Pontchartrain, the flow circulation and sediment transport are most important key tasks to be studied.

3. Model descriptions

To simulate the flow field and sediment transport in Lake Pontchartrain, a two-dimensional depth-averaged model, CCHE2D, was applied. CCHE2D is a 2D hydrodynamic and sediment transport model that can be used to simulate unsteady turbulent flows with irregular boundaries and free surfaces (Jia and Wang 1999, Jia et al. 2002). It is a finite element model utilizing a special method based on the collocation approach called the "efficient element method". This model is based on the 2D Reynolds-averaged Navier-Stokes equations. By

http://dx.doi.org/10.5772/54435

applying the Boussinesq approximation, the turbulent stress can be simulated by the turbulent viscosity and time-averaged velocity. There are several turbulence closure schemes available within CCHE2D, including the parabolic eddy viscosity, mixing length, k–ε and nonlinear k–ε models. In this model, an upwinding scheme is adopted to eliminate oscillations due to advection, and a convective interpolation function is used for this purpose due to its simplicity for the implicit time marching scheme which was adopted in this model to solve the unsteady equations. The numerical scheme of this approach is the second order. The velocity correction method is applied to solve the pressure and enforce mass conservation. Provisional velocities are solved first without the pressure term, and the final solution of the velocity is obtained by correcting the provisional velocities with the pressure solution. The system of the algebraic equations is solved using the Strongly Implicit Procedure (SIP) method (Stone 1968).

3.1. Governing equations

The free surface elevation of the flow is calculated by the continuity equation:

$$\frac{\partial h}{\partial t}+\frac{\partial uh}{\partial x}+\frac{\partial vh}{\partial y}=0 \tag{1}$$

The momentum equations for the depth-integrated two-dimensional model in the Cartesian coordinate system are:

$$\frac{\partial u}{\partial t}+u\frac{\partial u}{\partial x}+v\frac{\partial u}{\partial y}=-g\frac{\partial \eta}{\partial x}+\frac{1}{h}\left(\frac{\partial h\tau_{xx}}{\partial x}+\frac{\partial h\tau_{xy}}{\partial y}\right)+\frac{\tau_{sx}-\tau_{bx}}{\rho h}+f_{Cor}v \tag{2}$$

$$\frac{\partial v}{\partial t}+u\frac{\partial v}{\partial x}+v\frac{\partial v}{\partial y}=-g\frac{\partial \eta}{\partial x}+\frac{1}{h}\left(\frac{\partial h\tau_{yx}}{\partial x}+\frac{\partial h\tau_{yy}}{\partial y}\right)+\frac{\tau_{sy}-\tau_{by}}{\rho h}-f_{Cor}u \tag{3}$$

where u and v are the depth-integrated velocity components in x and y directions, respectively; t is the time; g is the gravitational acceleration; η is the water surface elevation; ρ is the density of water; h is the local water depth; f_{Cor} is the Coriolis parameter; τ_{xx}, τ_{xy}, τ_{yx} and τ_{yy} are depth integrated Reynolds stresses; and τ_{sx} and τ_{sy} are surface share stresses in x and y directions, respectively; and τ_{bx} and τ_{by} are shear stresses on the interface of flow and bed in x and y directions, respectively.

The turbulence Reynolds stresses in equations (2) and (3) are approximated according to the Bousinesq's assumption that they are related to the main rate of the strains of the depth-averaged flow field and an eddy viscosity coefficient ν_t which is computed using the Smagorinsky scheme (Smagorinsky 1993):

$$\nu_t = \alpha \Delta x \Delta y \left[\left(\frac{\partial u}{\partial x} \right)^2 + \frac{1}{2} \left(\frac{\partial v}{\partial x} + \frac{\partial u}{\partial y} \right)^2 + \left(\frac{\partial v}{\partial y} \right)^2 \right]^{1/2} \tag{4}$$

The parameter α ranges from 0.01 to 0.5. In this study, it was taken as 0.1.

In CCHE2D model, three approaches are adopted to simulate non-uniform sediment transport. One is the bed load transport, which is to simulate the bed load only without considering the diffusion of suspended load. The second approach is the suspended load transport, which simulates suspended load and treats bed -material load as suspended load. The third approach is to simulate bed load and suspended load separately (Jia and Wang 1999, Jia et al. 2002, Wu 2008).

In this study, CCHE2D was used to simulate sediment transport in Lake Pontchartrain during the BCS opening for flood release. In this period, sediment transport in the lake is primarily dominated by suspended sediment. So the second sediment transport approach, suspended load, was used for this study, and the non-uniform suspended sediment (SS) transport equation can be written as:

$$\frac{\partial c_k}{\partial t} + u \frac{\partial c_k}{\partial x} + v \frac{\partial c_k}{\partial y} = \frac{\partial}{\partial x} \left(D_{cx} \frac{\partial c_k}{\partial x} \right) + \frac{\partial}{\partial y} \left(D_{cy} \frac{\partial c_k}{\partial y} \right) + S_{ck} \tag{5}$$

Where c_k is the depth-averaged concentration of the kth size class of SS; D_{cx} and D_{cy} are the mixing coefficients of SS in x and y directions, respectively; S_{ck} is the source term and can be calculated by:

$$S_{ck} = -\frac{\alpha_t \omega_{sk}}{h} (c_k - c_{t*k}) \tag{6}$$

Where c_{t*k} is the equilibrium sediment concentration of the kth size class of suspended load; ω_{sk} is the settling velocity of the kth size class; α_t is the adaptation coefficient of suspended load, and it can be estimated using the formula proposed by Wu (2008).

Settling velocity is calculated using Zhang's formula (Zhang and Xie 1993):

$$w_{sk} = \sqrt{\left(13.95 \frac{\nu}{d_k} \right) + 1.09 \left(\frac{\gamma_s}{\gamma} - 1 \right) g d_k} - 13.95 \frac{\gamma}{d_k} \tag{7}$$

where ν is the kinematic viscosity; d_k is the diameter of the kth size class of sediment; γ_s and γ are the densities of water and sediment; g is the gravity acceleration.

http://dx.doi.org/10.5772/54435

The equilibrium sediment concentration c_{t*k} can be calculated based on sediment transport capacities of fractional suspended load and bed load. Based on field and laboratory data, Wu et al (2000) proposed a formula to calculate the fractional suspended load transport capacity φ_{sk} :

$$\varphi_{sk} = 0.0000262\left[\left(\frac{\tau}{\tau_{ck}} - 1\right)\frac{U}{\omega_{sk}}\right]^{1.74} \tag{8}$$

where U is the depth-averaged velocity; τ is the shear stress; τ_{ck} is the critical shear stress and can be calculated by

$$\tau_{ck} = 0.03(\gamma_s - \gamma)d_k\left(\frac{p_{hk}}{p_{ek}}\right)^{0.6} \tag{9}$$

in which p_{hk} and p_{ek} are the hiding and exposure probabilities for the k-th size class of sediment, they can be defined as:

$$p_{hk} = \sum_{j=1}^{N} p_{bj}\frac{d_j}{d_k + d_j} \tag{10}$$

$$p_{ek} = \sum_{j=1}^{N} p_{bj}\frac{d_k}{d_k + d_j} \tag{11}$$

where N is the total number of particle size classes in the non-uniform sediment mixture; p_{bj} is the probability of particles d_j staying in front of particles d_k. A relationship between p_{hk} and p_{ek} is known as:

$$p_{hk} + p_{ek} = 1 \tag{12}$$

In Eq. (8) φ_{sk} can also be expressed by:

$$\varphi_{sk} = \frac{q_{s*k}}{p_{bk}\sqrt{\left(\frac{\gamma_s}{\gamma} - 1\right)gd_k^3}} \tag{13}$$

in which p_{bk} is the bed material gradation; and q_{s^*k} is the equilibrium transport rate of the k-th size class of suspended load per unit width. Based on Eqs. (8) and (13), the following equation can be obtained to calculate q_{s^*k} :

$$q_{s^*k} = \varphi_{sk} p_{bk} \sqrt{\left(\frac{\gamma_s}{\gamma} - 1\right) g d_k^3} = 0.0000262 \left[\left(\frac{\tau}{\tau_{ck}} - 1\right) \frac{U}{\omega_{sk}}\right]^{1.74} p_{bk} \sqrt{\left(\frac{\gamma_s}{\gamma} - 1\right) g d_k^3} \tag{14}$$

Wu et al. (2000) also proposed a formula to calculate the fractional bed load transport capacity φ_{bk}:

$$\varphi_{bk} = 0.0053 \left[\left(\frac{n'}{n}\right)^{1.5} \frac{\tau}{\tau_{ck}} - 1\right]^{2.2} \tag{15}$$

where n is the Manning's roughness coefficient; n' is the Manning's coefficient corresponding to the grain roughness, $n' = d_{50}^{1/6} / 20$; the transport capacity φ_{bk} can also be expressed as:

$$\varphi_{bk} = \frac{q_{b^*k}}{p_{bk} \sqrt{\left(\frac{\gamma_s}{\gamma} - 1\right) g d_k^3}} \tag{16}$$

in which q_{b^*k} is the equilibrium transport rate of the k-th size class of bed load per unit width. Based on Eqs. (15) and (16), the following equation can be obtained to calculate q_{b^*k}:

$$q_{b^*k} = \varphi_{bk} p_{bk} \sqrt{\left(\frac{\gamma_s}{\gamma} - 1\right) g d_k^3} = 0.0053 \left[\left(\frac{n'}{n}\right)^{1.5} \frac{\tau}{\tau_{ck}} - 1\right]^{2.2} p_{bk} \sqrt{\left(\frac{\gamma_s}{\gamma} - 1\right) g d_k^3} \tag{17}$$

Based on Eqs.(14) and (17), the equilibrium sediment concentration c_{t^*k} in Eq. (6) can be calculated by:

$$c_{t^*k} = \frac{q_{s^*k} + q_{b^*k}}{Uh} = \frac{p_{bk} \sqrt{\left(\frac{\gamma_s}{\gamma} - 1\right) g d_k^3}}{Uh} \left\{ 0.0000262 \left[\left(\frac{\tau}{\tau_{ck}} - 1\right) \frac{U}{\omega_{sk}}\right]^{1.74} + 0.0053 \left[\left(\frac{n'}{n}\right)^{1.5} \frac{\tau}{\tau_{ck}} - 1\right]^{2.2} \right\} \tag{18}$$

The wind shear stresses (τ_{sx} and τ_{sy}) at the free surface are expressed by

http://dx.doi.org/10.5772/54435

$$\tau_{sx} = \rho_a C_d U_{wind} \sqrt{U_{wind}^2 + V_{wind}^2} \tag{19}$$

$$\tau_{sy} = \rho_a C_d V_{wind} \sqrt{U_{wind}^2 + V_{wind}^2} \tag{20}$$

where ρ_a is the air density; U_{wind} and V_{wind} are the wind velocity components at 10 m elevation in x and y directions, respectively. Although the drag coefficient C_d may vary with wind speed (Koutitas and O'Connor 1980; Jin et al. 2000), for simplicity, many researchers assumed the drag coefficient was a constant on the order of 10^{-3} (Huang and Spaulding 1995; Rueda and Schladow 2003; Chao et al 2004; Kocyigit and Kocyigit 2004). In this study, C_d was taken as 1.5×10^{-3}.

In this study, the decoupled approach was used to simulate sediment transport. At one time step, the flow fields, including water elevation, velocity components, and eddy viscosity parameters were first obtained using the hydrodynamic model, and then the suspended sediment concentration was solved numerically using Eq. (5).

4. Model verification

4.1. Tide-induced flow

A comparison of model simulation to an analytical solution was performed for a tidally forced flow in a square basin with constant water depth and no bottom friction. It was assumed that right side of the basin is an open boundary, and the other three sides are the closed solid wall. The tidal flow was simulated by driving the free surface elevation at the open boundary of the basin. A standing cosine wave with the maximum amplitude of A_m at the open boundary was introduced. This case has been used by other researchers to verify their models (Huang and Spaulding 1995; Zhang and Gin 2000). The analytical solution for surface elevation (ξ) and velocity (U) were given by Ippen (1966):

$$\xi = A_m \cos(\omega t) \tag{21}$$

$$U(x,t) = \frac{A_m \omega x}{H} \sin(\omega t) \tag{22}$$

in which A_m is the tide amplitude; ω is the angular frequency, $\omega = 2\pi / T$; T is the tidal period; t is the time; x is the distance from the left closed basin boundary; U is the velocity in x direction; and H is the base water depth. In the numerical simulation, the following values were adopted: basin length is 12km, width is 12km, H=10m, T=12h, A_m=0.5m. Figs.2 and 3 show the comparison of the analytical solution and the numerical simula-

tion results for water surface elevation and velocity. The numerical results are in good agreement with analytical solutions.

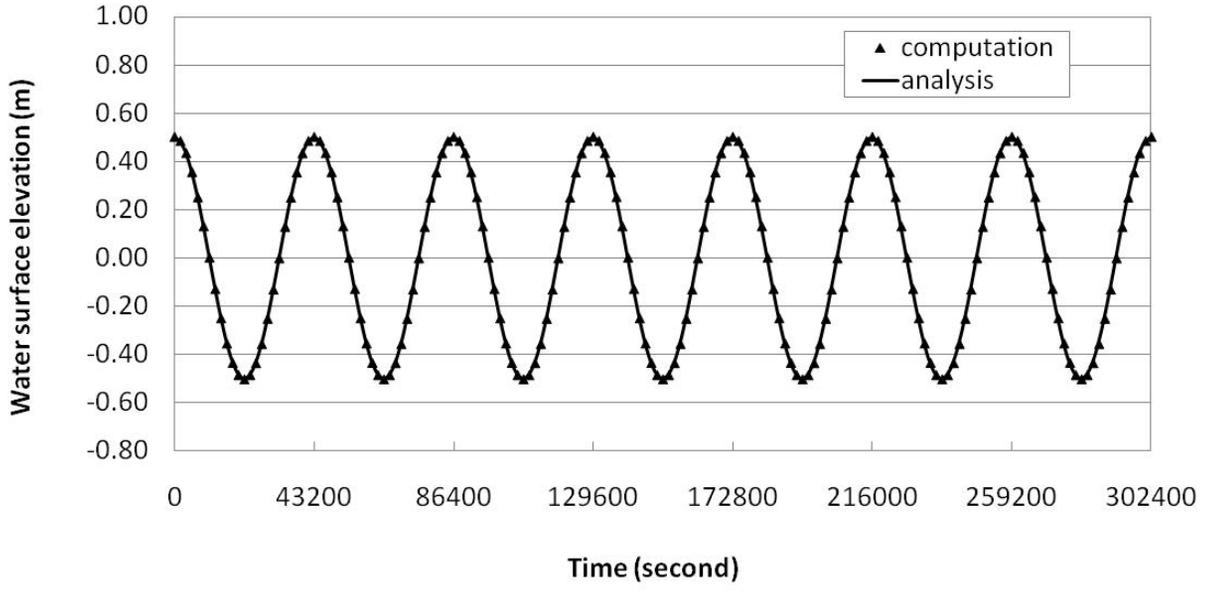

Figure 2. Comparison of analytical solution and numerical simulation for water surface elevation

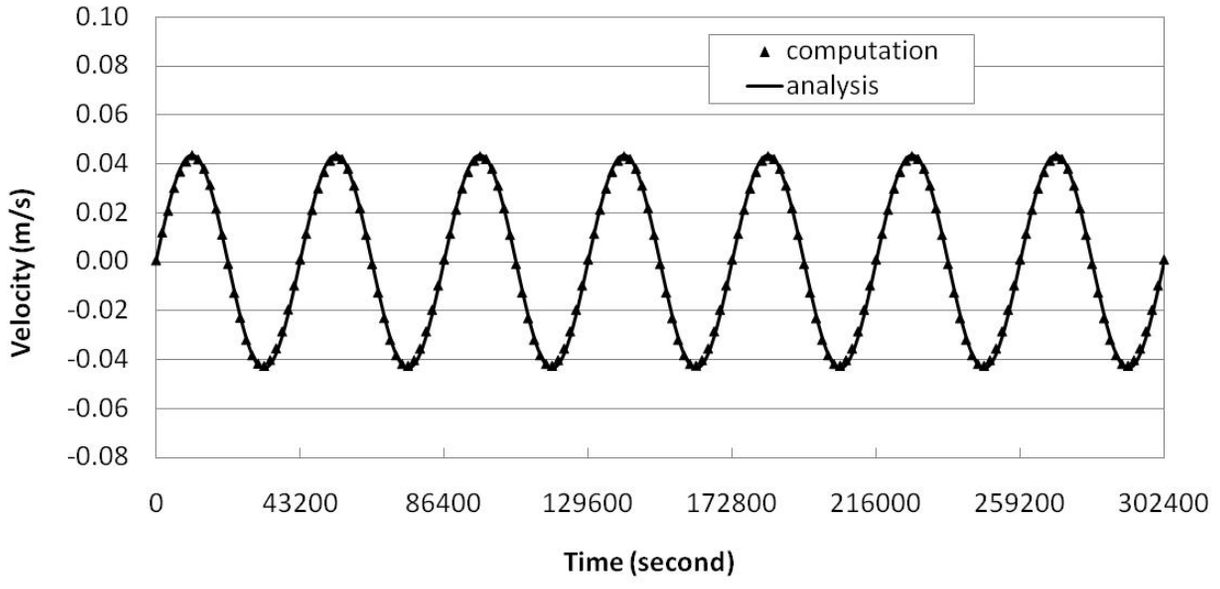

Figure 3. Comparison of analytical solution and numerical simulation for depth-averaged velocity

http://dx.doi.org/10.5772/54435

4.2. Verification of mass transport

To verify the transport simulation model, the numerical results were tested against an analytical solution for predicting salinity intrusion in a one-dimensional river flow with constant depth. It was assumed that the downstream end of the river is connected with the ocean with salt water. At the end of the river reach (x=0), there is a point source with a constant salinity, S_0, from the ocean, and the salt water may intrude into the river due to dispersion (Fig.4). Under the steady-state condition, the salinity in the river can be expressed as:

$$U\frac{\partial S}{\partial x} = D_x \frac{\partial^2 S}{\partial x^2} \tag{23}$$

where U is the velocity (no tidal effect); S is the salinity in river; D_x is the dispersion coefficient; and x is the displacement from downstream seaward boundary (point O). An analytical solution given by Thomann and Mueller (1988) is:

$$S(x) = S_0 \exp(\frac{Ux}{D_x}) \tag{24}$$

in which S_0 is the salinity at downstream seaward boundary. In this test case, it was assumed that the water depth = 10 m, U=0.03m/s, D_x=30 m^2/s, and S_0 = 30 ppt. Fig. 5 shows the salinity concentration distributions obtained by the numerical model and analytical solution. The maximum error between the numerical result and analytical solution is less than 2%.

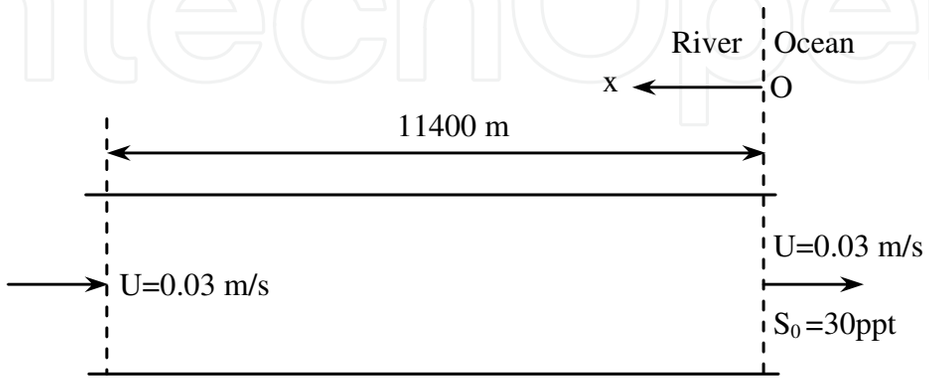

Figure 4. Test river for model verification

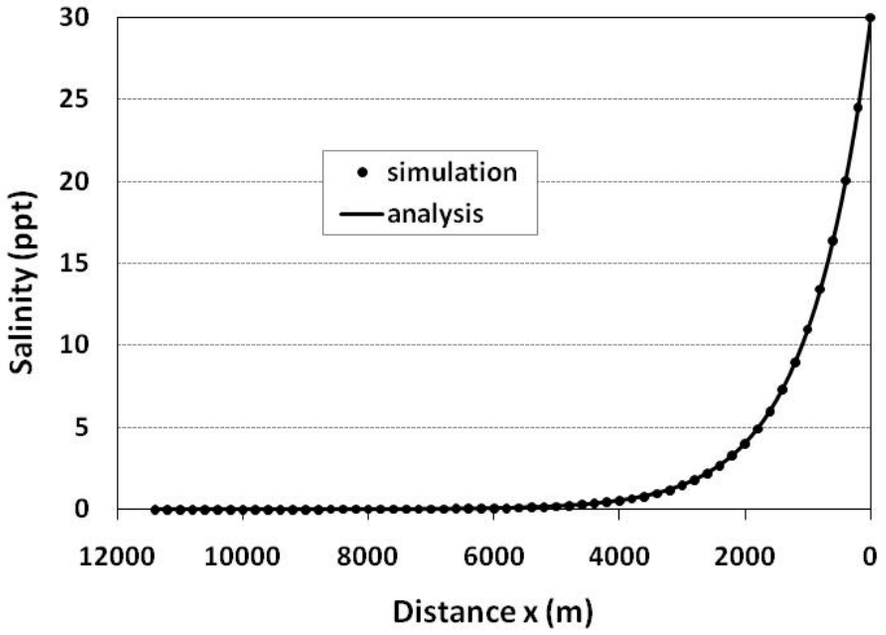

Figure 5. Salinity distribution along the river

5. Model application to lake pontchartrain

5.1. Study area

Fig. 6 shows the bathymetry and locations of field measurement stations of the study site — Lake Pontchartrain. The circulation in Lake Pontchartrain is an extremely complicated system. It is affected by tide, wind, fresh water input, etc. The lake has a diurnal tide with a mean range of 11 cm. Higher salinity waters from the Gulf of Mexico can enter the lake through three narrow tidal passes: the Rigolets, Chef Menteur, and a man-made Inner Harbor Navigation Canal (IHNC). Freshwater can discharge into the lake through the Tchefuncte and Tangipahoa Rivers, the adjacent Lake Maurepas, and from other watersheds surrounding the lake. The Bonnet Carré Spillway (BCS) is located at the southwest of the lake.

Based on the bathymetric data, the computational domain was descritized into an irregular structured mesh with 224×141 nodes using the NCCHE Mesh Generator (Zhang and Jia, 2009).

5.2. Boundary conditions

As shown in Fig.6, there are two inlet boundaries located at the northwest of the lake, and three tidal boundaries located at the south and east of the lake. The flow discharges at Tchefuncte and Tangipahoa Rivers obtained from USGS were set as two inlet boundary condi-

http://dx.doi.org/10.5772/54435

tions. The hourly water surface elevation data at the Rigolets Pass obtained from USGS was set as a tidal boundary. Due to the lack of measured surface elevation data at Chef Menteur Pass, the Rigolets data was used (McCorquodale et al., 2005). After the BCS was opened for flood release, the flow discharge at BCS was set as inlet boundary conditions.

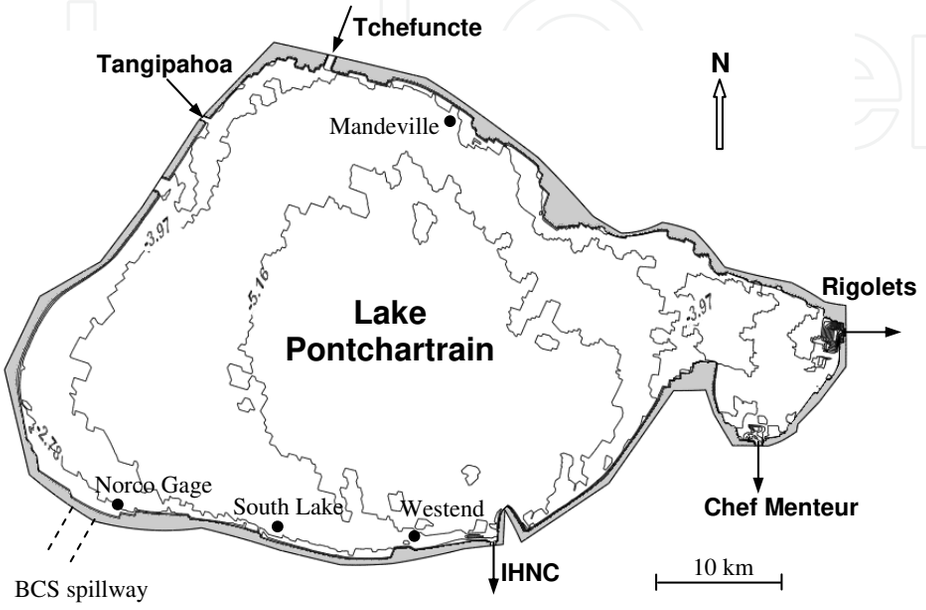

Figure 6. The bathymetry and field measurement stations in Lake Pontchartrain

The other tidal pass, IHNC, is a man-made canal which connects the Lake Pontchartrain and Mississippi River with a lock structure. It is also connected with both the Gulf Intracoastal Waterway and the Mississippi River Gulf Outlet (MRGO). The measured daily water surface elevation data is the only available data at IHNC. In general, the daily water surface elevation data can not represent the variations of tidal boundary. It would cause problems if the measured daily data was directly set as tidal boundary conditions at IHNC. To resolve this problem, the relationship between measured daily water surface elevations at Rigolets and IHNC tidal passes were established and adopted to convert the hourly data at Rigolest to the hourly data at IHNC. Since both IHNC and Rigolets tidal passes are connected with the Gulf of Mexico, the tide effects at these two places are assumed to be similar. By comparing the measured daily water surface elevations at Rigolets and IHNC, no obvious phase differences were observed (McCorquodale et al., 2005). Fig.7 shows the comparison of measured daily water surface elevations at Rigolets and IHNC tidal passes.

The measured results show that the surface elevations at the two locations have a close linear relation with the correlation coefficient r^2 being 0.92:

$$\eta_i = 1.0484\eta_r - 0.0055 \tag{25}$$

Where η_i and η_r are the daily surface elevations at IHNC and Regolets, respectively. It was assumed that the hourly water surface elevations at IHNC and Regolets have the similar relationships, and Eq. (25) was adopted to calculate the hourly water surface elevations at IHNC from the measured hourly surface elevation at Rigolets. The calculated hourly data was plotted together with the measured daily data at IHNC (Fig.8), a similarity distribution was observed. So the calculated hourly surface elevation was used as tidal boundary condition at IHNC.

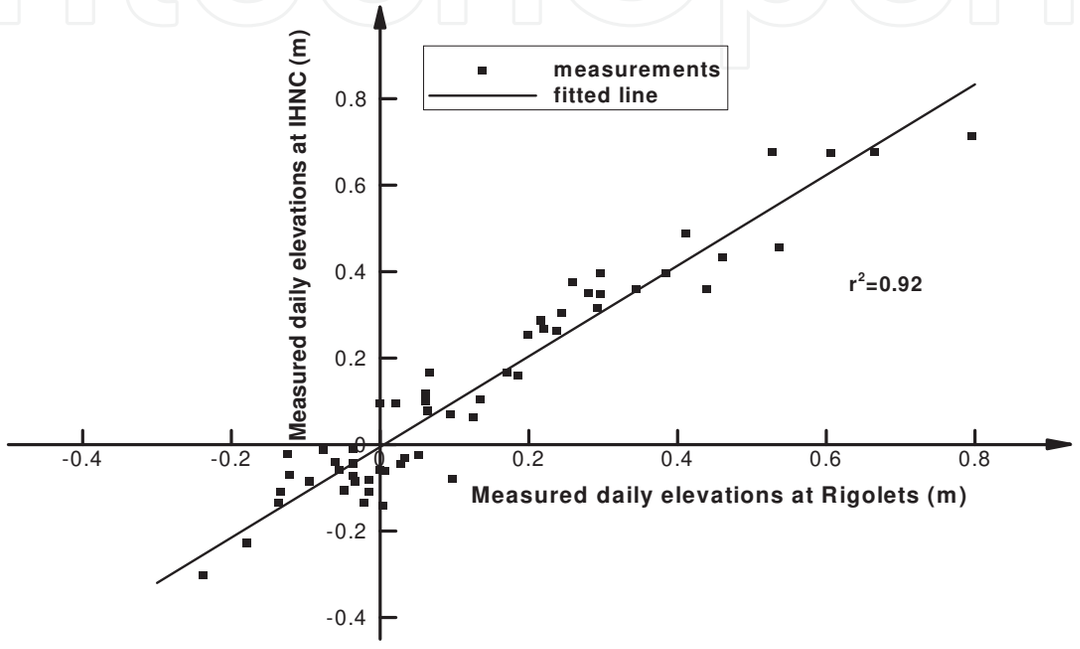

Figure 7. Comparison of measured daily water surface elevations at Regolets and IHNC

5.3. Model calibration

After obtaining the inlet boundaries, outlet boundaries, and wind speeds and directions, the developed model was applied to simulate the flow circulation and sediment transport in Lake Pontchartrain. Some field measured data sets were used for model calibration and validation.

A period from March 1 to 31, 1998, was selected for model calibration. For calibration runs, several parameters, such as drag coefficient C_d, Manning's roughness coefficient, and the parameter α in Smagorinsky scheme (Eq.4), were adjusted to obtain a reasonable reproduction of the field data. In this study, C_d = 0.0015, Manning's roughness coefficient = 0.025, and α = 0.1. Simulated water surface elevations and depth-averaged velocities were compared with the field measured data. Fig. 9 shows the simulated and measured water surface elevations at the Mandeville. Fig. 10 and Fig.11 show the simulated and measured depth-averaged velocities in x and y directions at the South Lake Site, respectively.

http://dx.doi.org/10.5772/54435

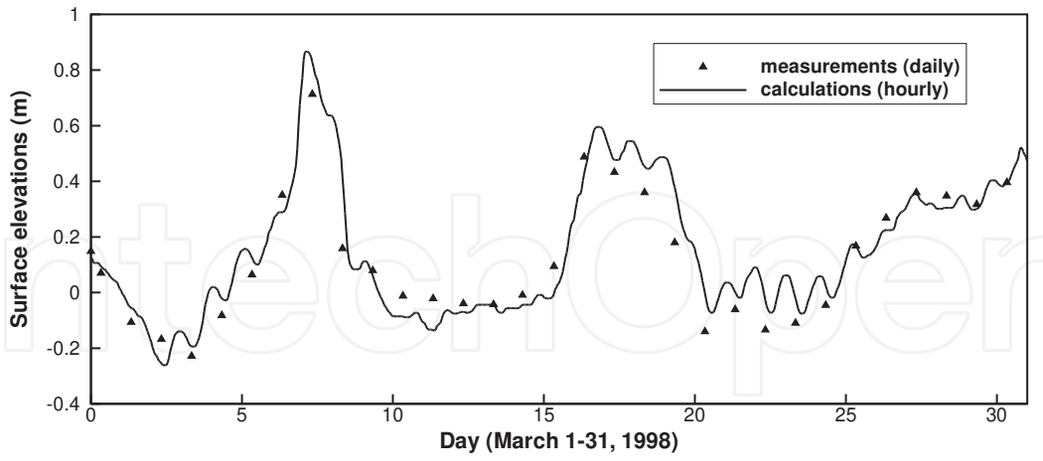

Figure 8. The calculated hourly water surface elevation at IHNC using Eq. (25)

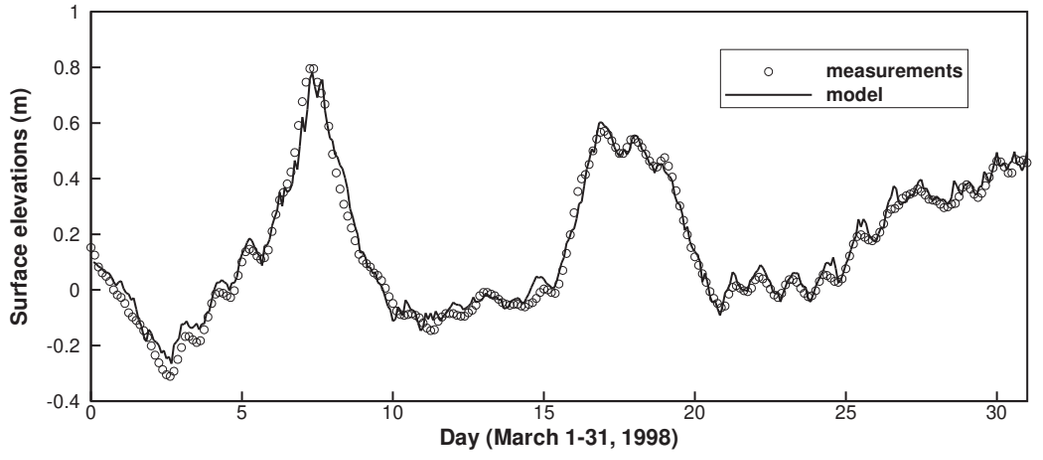

Figure 9. Simulated and measured water surface elevations at the Mandeville Station

A set of statistics error analysis, including root mean square error (RMSE), relative RMSE (RMSE/range of observed data) and correlation coefficient (r^2), were used to assess the performance of the model for the calibration case (Table 2). The RMSE between simulated and observed water surface elevations at Mandeville Station was 0.037m and the relative RMSE of water surface elevations at this station was 3.4%. The r^2 of simulated and observed water surface elevations at this station was 0.98. The measured velocity data set at South Lake station was used for model comparison. It can be observed that the RMSE of u-velocity and v-velocity were 0.044 m/s and 0.019 m/s. The relative RMSE for u-velocity and v-velocity were 15% and 12%; and r^2 of simulated and observed u-velocity and v-velocity were 0.52 and 0.41, respectively. In general, the flow fields produced by the numerical model are in agreement with field measurements.

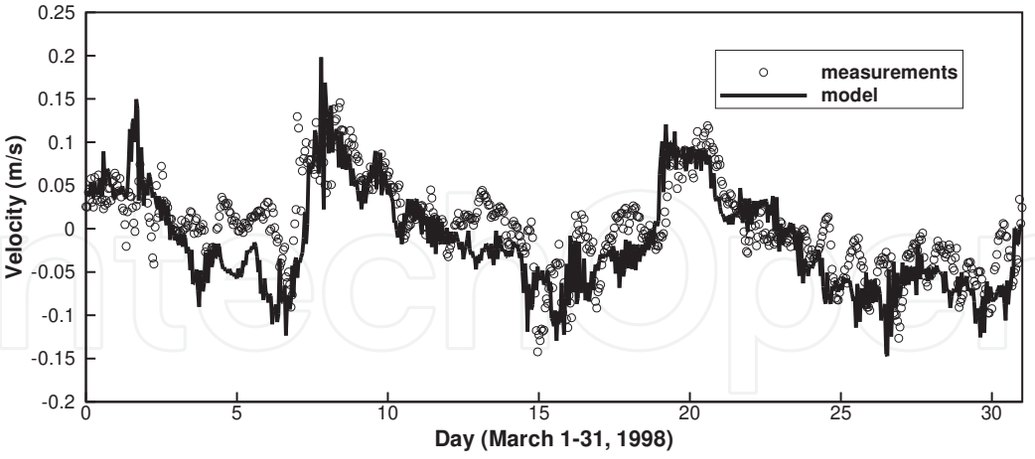

Figure 10. Simulated and measured depth-averaged velocities in west-east direction at the South Lake Site

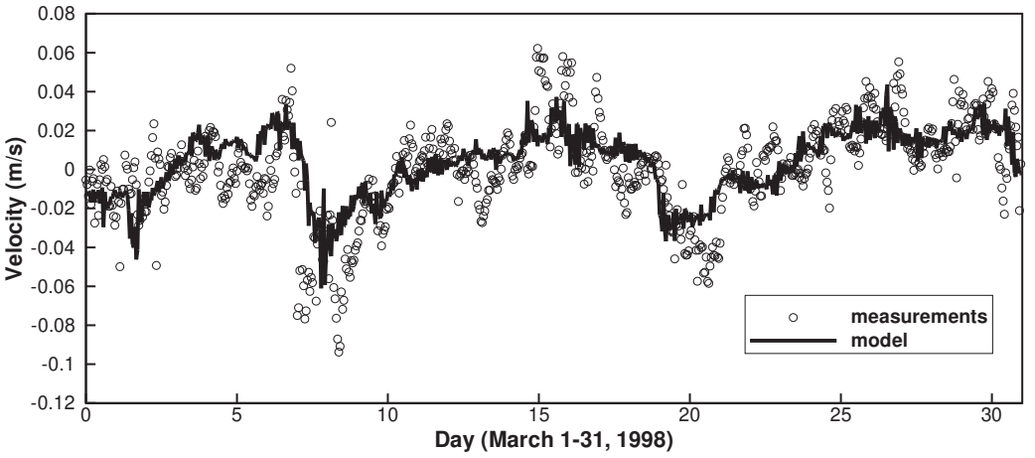

Figure 11. Simulated and measured depth-averaged velocities in south-north direction at the South Lake Site

Station	Variable	RMSE	Observed range	Relative RMSE	r^2
Mandeville	Water level	0.037 m	1.11 m	3.40%	0.98
South Lake	u-velocity	0.044 m/s	0.29 m/s	15%	0.52
South Lake	v-velocity	0.019 m/s	0.16 m/s	12%	0.41

Table 2. Statistics error analysis of the model calibration case

5.4. Modeling the suspended sediment during the BCS opening for 1997 flood release

After the Bonnet Carré Spillway (BCS) was built to divert Mississippi River flood waters to the Gulf of Mexico via Lake Pontchartrain, there were 10 times opening events occur-

http://dx.doi.org/10.5772/54435

red from 1937 to 2011. In this study, the 1997 flood release event was selected for model simulation.

In 1997, the BCS was opened for flood release from 3/17 to 4/18. The maximum flow discharge was about 6881 m^3/s, and over 31 days of flood release. The average discharge was about 4358 m^3/s. Fig. 12 shows the flow hydrograph at the spillway (Department of Natural Resources, 1997; McCorquodale et al. 2007). The total volume of sediment-laden water entering Lake Pontchartrain was approximately 1.18×10^{10} m^3, or twice the volume of the lake (Turner et al., 1999). The total amount of sediment entering the lake was about 9.1 million tons, more than 10 times as much as the normal yearly sediment loads of the lake. The suspended sediment (SS) concentration at the spillway gate was about 240 mg/l (Manheim and Hayes, 2002).

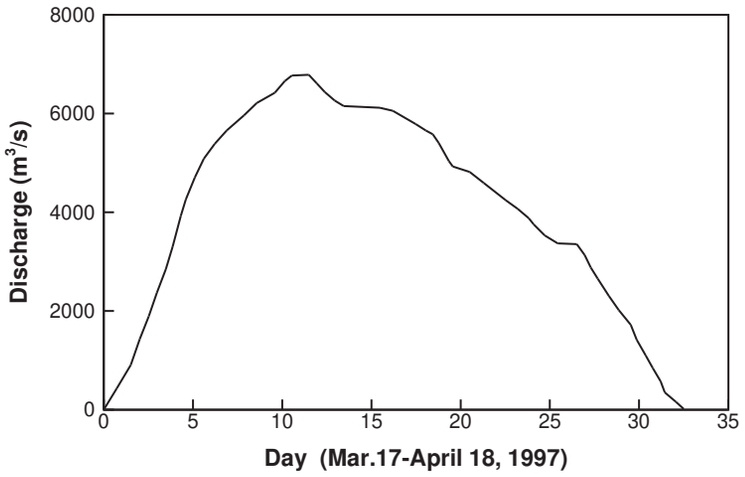

Figure 12. The flow hydrograph at the Bonnet Carré Spillway during the 1997 event

The calibrated CCHE2D model was applied to simulate the lake flow fields and sediment transport during the BCS opening in 1997. In this period, the flow discharge was very strong, and the "suspended load approach" was adopted for simulating sediment transport in the lake. The observed flow discharge was set as inlet boundary condition at BCS. The water surface elevations at Rigolets and Chef Menteur were set as tidal boundaries. The wind speeds and directions at the New Orleans International Airport were used for model simulation. The observed SS concentration was set as inlet sediment boundary condition at BCS. In general, the sediment in Lake Pontchartrain is cohesive sediment. However, during the BCS opening, sediment concentration in Lake Pontchartrain is dominated by the sediment coming from the Mississippi River. It was assumed that the effect of sediment cohesion on suspended sediment transport is not significant. Due to the lack of measured sediment data, the classes of non-uniform sediment size at BCS were estimated based on the observed sediment data in the lower Mississippi River (Thorne et al. 2008). Four size classes, including 0.005mm, 0.01mm, 0.02mm and 0.04mm were assumed to represent the non-uniform sizes of suspended sediment discharged into the lake from BCS. The fall velocity of

each size class of sediment was calculated using the Eq. (7) proposed by Zhang and Xie (1993). During this period, the flow discharge over the spillway dominated the lake hydrodynamics and suspended sediment transport. The bottom shear stress due to water flow as well as wind driven flow were obtained using the hydrodynamic model. The critical shear stress was calculated using Eq. (9) proposed by Wu (2008). The equilibrium sediment concentration c_{t^*k} was calculated using Eq. (18).

Fig. 13 shows the computed flow circulations in Lake Pontchartrain during the BCS opening. Due to the flood release, the entire lake water were moved eastward through Rigolets and Chef Menteur into the Gulf of Mexico, which was completely different from the flow patterns induced by tide and wind. Fig. 14 shows the comparisons of SS concentration obtained from the numerical simulation and remote sensing imageries (AVHRR data) provided by NOAA. The simulated SS concentrations are generally in good agreement with satellite imageries. The transport processes of SS in the lake were reproduced by the numerical model. The simulated results and satellite imageries revealed that a large amount of sediment discharged into the lake, moved eastward along the south shore and gradually expanded northward, eventually affecting the entire Lake after one month of diversion.

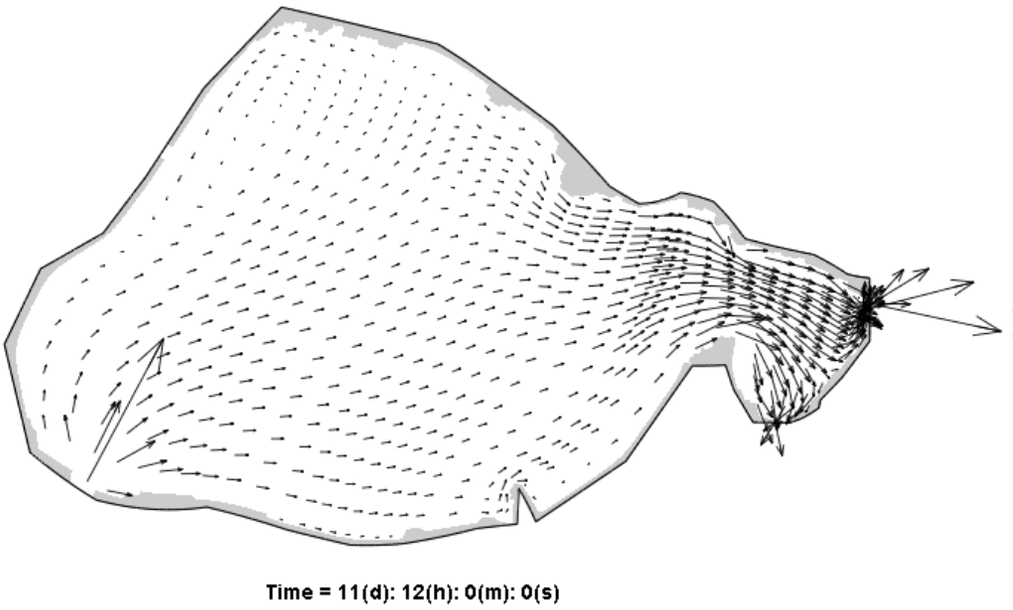

Figure 13. Flow circulations in Lake Pontchartrain during BCS opening in 1997

http://dx.doi.org/10.5772/54435

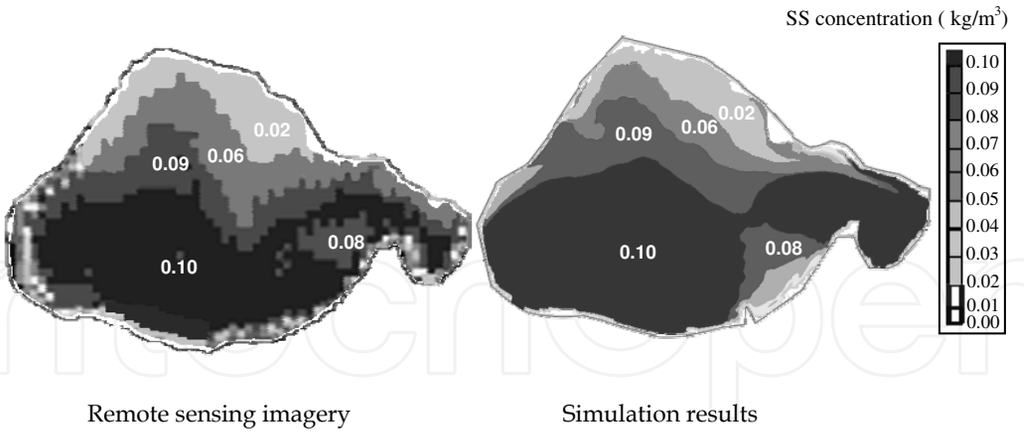

Figure 14. Comparisons of simulated depth-averaged SS concentration and remote sensing imageries (4/7/1997)

6. Discussion

In general, wind and tide are the major driving mechanisms of circulation in Lake Pontchartrain. When the tidal level changes, most of the water that enters or leaves the lake must come through the three narrow tidal passes at the east and south end of the lake. Since the tidal passes are very narrow, the tidal force may affect the flow fields near the tidal passes. When the wind blows over the lake, it may affect flow circulations of the whole lake. Fig. 15 shows the general flow pattern of the lake induced by tide and wind. It was completely different from the one when the BCS was opened for flood release and caused the entire lake water to be moved eastward into the Gulf of Mexico (Fig. 13). Due to the effects of tide and wind, the stronger currents occur along the shoreline where the water depth is shallow and near the narrow tidal passes, and weaker currents are in the center of the lake. These results are similar to results obtained by other researchers (Signell and List 1997, McCorquodale et al., 2005).

Under the normal condition, sediment in Lake Pontchartrain is dominated by cohesive sediments except for a small number of areas near the river mouths and tidal passes (Flocks et al. 2009). In response to wind and tidal induced flow shown in Fig. 15, sediment may transport/resuspend near shoreline and tidal passes, and deposit in the lake center.

During the BCS opening for flood release in 1997, large amount of sediment discharged from the Mississippi River into Lake Pontchartrain. Sediment transport in Lake Pontchartrain is dominated by the suspended sediment from the Mississippi River, and the effect of sediment cohesion can be ignored. In this period, the flow fields were majorly determined by the flow discharge at the BCS. They were also affected by the wind and tide induced flows. The simulated results and satellite imageries indicated that the suspended sediment moved eastward along the south shore first, gradually expanded northward, and was distributed throughout almost the entire lake about three weeks after the BCS opening. It was reported due to the flood release, a significant amount of nutrients were discharged into

Lake Pontchartrain, which may result in a massive algal bloom in the lake. However, the sediment and nutrients were simultaneously discharged into the lake, and the algae growth rate was restricted as a result of extremely high suspended sediment concentration in the lake (Chao et al 2007). So there was no algal bloom observed in the lake during the BCS opening. After the BCS was closed, the sediment derived from the Mississippi River gradually dispersed in the water column and deposited to the lake bed. In response to the low SS concentration, high nutrients, temperature and light intension, the algal bloom occurred in a large area of the lake, and the peak of the algal bloom observed in mid-June, about two months after the spillway closure (Dortch et al., 1998). In general, after the BCS was closed, it took about two to three months for the SS concentration in the lake recovered to the seasonal average level.

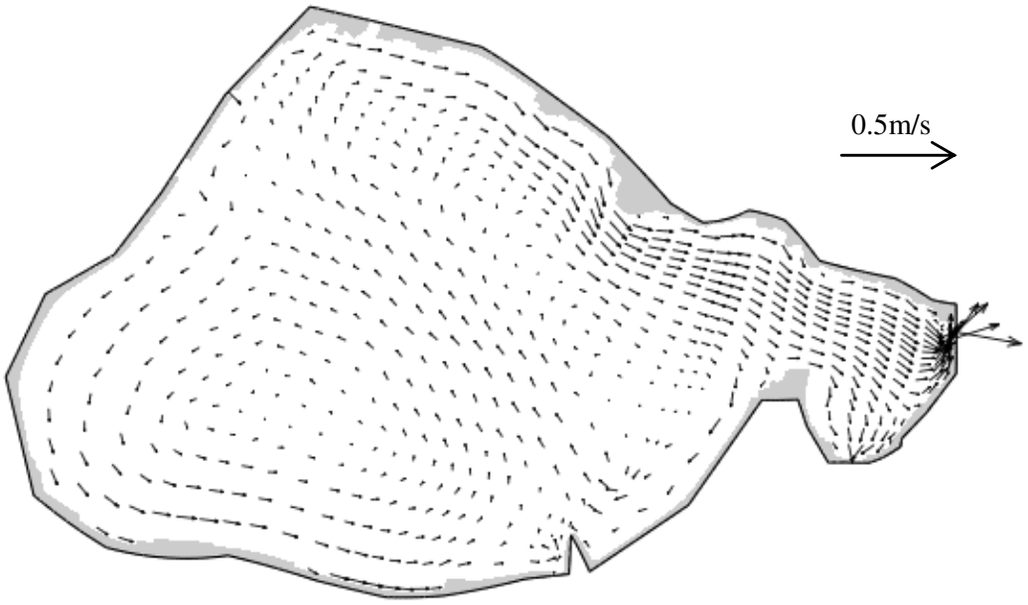

Figure 15. General flow circulations in Lake Pontchartrain due to tide and wind

7. Conclusions

A numerical model was applied to simulate the flow circulations and suspended sediment transport in Lake Pontchartrain in Louisiana, under tide, wind and flood release. It is one of the most significant real life problems we can find with reasonable field measurements obtained from USGS and USACE. Additional satellite imageries were obtained from NOAA for model validation. The results of these comparisons are in good agreement within the accuracy limitations of both the approximate numerical model solutions and the field measurements under the difficult conditions.

In the BCS flood release event, a vast amount of fresh water, sediment and nutrients were discharged into Lake Pontchartrain. The dispersion and transport processes of the suspend-

http://dx.doi.org/10.5772/54435

ed sediment in the lake were simulated successfully using the numerical model. The simulated SS concentrations are generally in good agreement with satellite imageries provided by NOAA. The differences of flow circulation and sediment transport in the lake under normal condition and BCS opening event were discussed. The simulated results and satellite imageries show that after the BCS opening, a large amount of sediment discharged into the lake, moved eastward and gradually expanded northward, eventually affecting the entire lake. After the BCS closure, the sediment derived from the Mississippi River gradually deposited to the lake bed and it took two to three months for the SS concentration in the lake recovered to the seasonal average level.

This research effort has positively demonstrated that the numerical model is capable of predicting free surface flow and sediment transport in Lake Pontchartrain under extreme natural conditions. It is a useful tool for providing information on hydrodynamics and sediment transport in such a big lake where the field measurements may not be sufficient. All the information obtained from the numerical model is very important for lake restoration and water quality management.

Acknowledgements

This research was funded by the US Department of Homeland Security and was sponsored by the Southeast Region Research Initiative (SERRI) at the Department of Energy's Oak Ridge National Laboratory. The authors would like to thank Rich Signell and David Walters of the USGS, and George Brown of the USACE for providing field measured data in Lake Pontchartrain. The technical assistance from Yaoxin Zhang, Weiming Wu and suggestions and comments provided by Yan Ding, Tingting Zhu and Kathy McCombs of the University of Mississippi are highly appreciated.

Author details

Xiaobo Chao, Yafei Jia and A. K. M. Azad Hossain

The University of Mississippi, USA

References

[1] Chao, X, Jia, Y, & Shields, D. (2004). Three dimensional numerical simulation of flow and mass transport in a shallow oxbow lake. Proc., World Water & Environmental Resources Congress 2004, ASCE, Resyon, Va. (CD-Rom).

[2] Chao, X, Jia, Y, & Zhu, T. (2006). CCHE_WQ Water Quality Module. Technical Report : NCCHE-TR-The University of Mississippi., 2006-01.

[3] Chao, X, Jia, Y, Shields, D, & Wang, S. S. Y. (2007). Numerical Modeling of Water Quality and Sediment Related Processes. *Ecological Modelling*, 201, 385-397.

[4] Department of Natural Resources(1997). Bonnet Carre Spillway Opening. Hydrographic Data Report, Final Report.

[5] Dortch, M. S, Zakikhani, M, Kim, S. C, & Steevens, J. A. (2008). Modeling water and sediment contamination of Lake Pontchartrain following pump-out of Hurricane Katrina floodwater. Journal of Environmental ManagementS: , 429-442.

[6] Dortch, Q, Peterson, J, & Turner, R. (1998). Algal bloom resulting from the opening of the Bonnet Carre spillway in 1997. Fourth Bi-annual Basics of the Basin Symposium. United States Geological Survey, , 28-29.

[7] Flocks, J, Kindinger, J, Marot, M, & Holmes, C. (2009). Sediment characterization and dynamics in Lake Pontchartrain, Louisiana. Journal of Coastal ResearchSpecial , 54(54), 113-126.

[8] Gulf Engineers & Consultants (GEC) ((1998). Biological and Recreational Monitoring of the Impacts of 1997 Opening of the Bonnet Carré Spillway Southeastern Louisiana. Final Report to U.S Army Corps of Engineers, New Orleans, Louisiana.

[9] Hamilton, G. D, Soileau, C. W, & Stroud, A. D. (1982). Numerical modeling study of Lake Pontchartrain. Journal of the Waterways, Port, Coastal and Ocean Division, ASCE. , 108, 49-64.

[10] Hossain, A, Jia, Y, Ying, X, Zhang, Y, & Zhu, T. T. (2011). Visualization of Urban Area Flood Simulation in Realistic 3D Environment, Proceedings of 2011 World Environmental & Water Resources Congress, May Palm Springs, California., 22-26.

[11] Huang, W, & Spaulding, M. (1995). 3D model of estuarine circulation and water quality induced by surface discharges. *Journal of Hydraulic Engineering*, 121(4), 300-311.

[12] Ippen, A. T. (1966). Estuary and Coastline Hydrodynamics. McGraw Hill, New York.

[13] Kocyigit, M. B, & Kocyigit, O. (2004). Numerical study of wind-induced currents in enclosed homogeneous water bodies. Turkish J. Engineering & Environmental Science, , 28, 207-221.

[14] Koutitas, C, & Connor, O. B., ((1980). Modeling three-dimensional wind-induced flows. ASCE, Journal of Hydraulic Division, 106 (11), 1843-1865.

[15] Jia, Y, & Wang, S. S. Y. (1999). Numerical model for channel flow and morphological change studies. *Journal of Hydraulic Engineering*, 125(9), 924-933.

[16] Jia, Y, Wang, S. Y. Y, & Xu, Y. (2002). Validation and application of a 2D model to channels with complex geometry. *International Journal of Computational Engineering Science*, 3(1), 57-71.

[17] Jin, K. R, Hamrick, J. H, & Tisdale, T. (2000). Application of three dimensional hydrodynamic model for Lake Okeechobee. J. Hydraulic Engineering, 126(10), , 758 EOF-772 EOF.

[18] Manheim, F. T, & Hayes, L. (2002). Sediment database and geochemical assessment of Lake Pontchartrain Basin, in Manheim FT, and Hayes L (eds.), Lake Pontchartrain Basin: Bottom Sediments and Related Environmental Resources: U.S. Geological Survey Professional Paper 1634.

[19] Mccorquodale, J. A, Georgiou, I, Chilmakuri, C, Martinez, M, & Englande, A. J. (2005). Lake Hydrodynamics and Recreational Activities in the South Shore of Lake Pontchartrain, Louisiana. Technical Report for NOAA, University of New Orleans.

[20] Mccorquodale, J. A, Georgiou, I, Retana, A. G, Barbe, D, & Guillot, M. J. (2007). Hydrodynamic modeling of the tidal prism in the Pontchartrain Basin, Technical report, The University of New Orleans.

[21] Mccorquodale, J. A, Roblin, R. J, Georgiou, I, & Haralampides, K. A. (2009). Salinity, nutrient, and sediment dynamics in the Pontchartrain Estuary. Journal of Coastal ResearchSpecial , 54(54), 71-87.

[22] Penland, S., Beall, A. and Kindinger, J. (2002). Environmental Atlas of the Lake Pontchartrain Basin. USGS Open File Report 02-206.

[23] Rueda, F.J. and Schladow, S.G. (2003). Dynamics of large polymictic lake. II: Numerical Simulations. Journal of Hydraulic Engineering. 129(2): 92-101.

[24] Signell, R.P. and List, J.H. (1997). Modeling Waves and Circulation in Lake Pontchartrain. Gulf Coast Association of Geological Societies Transactions. 47: 529-532.

[25] Smagorinsky, J. (1993). Large eddy simulation of complex engineering and geophysical flows, in Evolution of Physical Oceanography, edited by B. Galperin, and S. A. Orszag, pp. 3-36. Cambridge University Press.

[26] Stone, H.L. (1968). Iterative solution of implicit approximation of multidimensional partial differential equations. SIAM (Society for Industrial and Applied Mathematics) Journal on Numerical Analysis. 5: 530–558.

[27] Thomann, R.V. and Mueller, J.A. (1988). Principles of Surface Water Quality Modeling and Control. Harper&Row Publication, New York.

[28] Thorne, C., Harmar, O., Watson, C., Clifford, N., Biedenham, D. and Measures, R. (2008). Current and Historical Sediment Loads in the Lower Mississippi River. Final Report, Department of Geology, Nottingham University.

[29] Turner, R.F., Dortch, Q. and Rabalais, N.N. (1999). Effects of the 1997 Bonnet Carré Opening on Nutrients and Phytoplankton in Lake Pontchartrain. Final report submitted to the Lake Pontchartrain Basin Foundation, 117 p.

[30] United States Army Corps of Engineers (USACE) (2011). Bonnet Carre Spillway overview, Spillway pace (http://www.mvn.usace.army.mil/bcarre/2011operation.asp).

[31] Wu, W. (2008). Computational River Dynamics, Taylor & Francis Group, London, UK.

[32] Wu, W., Wang, S.S.Y. and Jia, Y. (2000). Non-uniform sediment transport in alluvial river, Journal of Hydraulic Research, IAHR 38 (6) 427-434.

[33] Zhang, Q.Y. and Gin, K.Y.H. (2000). Three-dimensional numerical simulation for tidal motion in Singapore's coastal waters. Coastal Engineering. 39: 71–92.

[34] Zhang, R.J. and Xie, J.H. (1993). Sedimentation Research in China, Systematic Selections. Water and Power Press. Beijing, China.

[35] Zhang, Y, & Jia, Y. (2009). CCHE Mesh Generator and User's Manual, Technical Report No. NCCHE-TR-University of Mississippi., 2009-1.

[36] Zhu, T, Jia, Y, & Wang, S. S. Y. (2008). CCHE2D water quality and chemical model capabilities. World Environmental and Water Resources Congress. Hawaii (CD-ROM).

IntechOpen